



A New Approach to Well-Defined, Stable and Site-Isolated Catalysts

K. Kovnir¹, M. Armbrüster^{1,2*}, D. Teschner², T. Venkov², F.C. Jentoft², A. Knop-Gericke², Yu. Grin¹, R. Schlögl²

¹ Max-Planck-Institut für Chemische Physik fester Stoffe, Nöthnitzer Str. 40, 01187 Dresden, Germany

² Department of Inorganic Chemistry, Fritz-Haber-Institute of the MPG, Faradayweg 4-6, 14195 Berlin, Germany

* Corresponding author: e-mail research@armbruester.net, Tel.: +44(0)1223/336533 Fax: +44(0)1223/336362
Current address: University of Cambridge Chemistry Department Lensfield Road Cambridge CB2 1EW United Kingdom

Received 29 March 2007; revised 13 May 2007; accepted 22 May 2007. Available online 8 August 2007.

Abstract

A new concept to circumvent some of the problems that are hindering a rational metallic catalyst development is introduced. Investigation of conventional metal catalysts – which consist of supported metals, metal mixtures or alloys – is handicapped by the presence of a variety of active sites, their possible agglomeration, metal-support interactions as well as segregation of the components. In order to avoid most of the drawbacks we employ well defined, ordered and *in-situ* stable unsupported intermetallic compounds. The knowledge of the chemical bonding in the compounds and the defined neighbourhood of the active sites allow a rational approach to catalysts with excellent selectivity as well as long-term stability. The concept is demonstrated for the intermetallic compound PdGa which is applied as catalyst for the selective hydrogenation of acetylene to ethylene.

1. Introduction

Because the terms “intermetallic compound” and “alloy” are often mixed up in the literature we will start by defining the two terms. Hereafter, an “intermetallic compound” is a chemical compound of two or more metallic elements and adopts an – at least partly – ordered crystal structure that differs from those of the constituent metals. Intermetallic compounds are single-phase materials and often hold a wide homogeneity range. On the other hand an “alloy” is a mixture of metals, intermetallic compounds and/or non-metals, thus, it can contain more than one phase.

The use of intermetallic compounds in catalysis (not as catalysts!) is widespread. The most well known examples are the Raney-type catalysts where an intermetallic compound – or an alloy – is leached in order to produce a high-surface area catalyst^[1,2]. During the leaching the intermetallic compound (e.g. NiAl₃^[3]) is decomposed resulting in the pure metal (very often Ni) as the catalytically active species.

In most of the other reports in which intermetallic compounds are used in catalysis they are decomposed during the catalytic reaction. A good and well explored exam-

ple is the hydrogenation of CO over RE-Ni and RE-Cu (RE = rare earth metal) intermetallic compounds which are decomposed *in-situ* to elemental nickel or copper particles and the corresponding rare earth oxide^[4-8].

Intermetallic compounds can also be formed *in-situ* due to strong metal-support interactions or by the reaction between different supported metallic species. Examples where strong metal-support interactions were detected are the selective hydrogenation of crotonaldehyde over Pt/ZnO^[9,10] and the steam reforming of methanol over Pd/ZnO^[11,12]. Under reaction conditions the intermetallic compounds PtZn and PdZn are formed and the high selectivity and activity is attributed to their presence.

In these cases (i.e. the decomposition or formation of intermetallic compounds *in-situ*) it is not easy to determine whether the intermetallic compound, the decomposition products and/or other components (e.g. the support) are catalytically active. This lack of knowledge prevents a rational development and improvement of these catalysts.

To circumvent these complications, our rational approach is based on the application of as pure as possible, stable and unsupported intermetallic compounds with ordered crystal structures as catalysts. The latter, in contrast to disordered alloys, leads to a uniform surrounding of the active sites, thus, the number of neighbouring sites as well

as the distance between them are known. By selecting intermetallic compounds with a suitable crystal structure, the active sites can be tailored to the needs of the reaction.

A reaction for which isolated active sites are needed, is the partial hydrogenation of acetylene in a large excess of ethylene – an important step in the purification of the ethylene feed for the production of polyethylene (industrial production $> 50 \cdot 10^6$ t/a). The reaction has to be highly selective to avoid the hydrogenation of ethylene while at the same time the concentration of acetylene has to be reduced from $\sim 1\%$ to the low ppm range to prevent the poisoning of the polymerization catalyst. It has been shown recently, that π -adsorbed ethylene can further be hydrogenated to ethane while di- σ adsorbed ethylene leads to ethylidyne and vinylidene species which do not desorb from the surface and cause deactivation.^[13–15] The isolation of Pd atoms will lead to increased stability of the catalysts due to suppressed carbon deposition. Additionally, absence of neighbouring Pd sites will significantly reduce the surface and sub-surface hydrogen supply which should improve the selectivity towards semi-hydrogenation.^[16] Thus, in order to obtain highly selective catalysts, neighbouring active sites have to be avoided. Applying our concept, we tested the intermetallic compound PdGa with isolated Pd atoms successfully as catalyst for the selective acetylene hydrogenation reaction – as will be shown later on.

It has already been pointed out, that the *in-situ* stability of the intermetallic compounds is crucial in order to connect the catalytic properties to the well-defined crystal structure. Since this is experimentally challenging and also time consuming, we employ quantum chemical methods beforehand, namely the electron localization function (ELF) and the electron localization indicator (ELI), to explore the bonding in the compounds^[17;18]. If covalent bonding (which corresponds to directed bonds, thus chemical stability) is revealed, the stability is investigated by different *in-situ* techniques. These include EXAFS to probe the short-range order, XRD to detect changes in the long-range order as well as XPS to monitor changes in the surface composition *in-situ*. Furthermore, the differences in the electronic structure to elemental Pd as well as the isolation of the active sites will be experimentally verified by XPS and FTIR spectroscopy. First results of this approach have been published elsewhere^[19;20].

2. Experimental

2.1. Preparation

PdGa was prepared by melting the appropriate amounts of the metals (Pd: ChemPur 99.95 %, Ga: ChemPur 99.99 %) under protective Ar atmosphere in a high frequency furnace (Hüttlinger TIG 5/300) and subsequent annealing of the ingot in an evacuated quartz glass ampoule at 1073 K for 170 h. The phase purity was controlled by X-ray powder diffraction (XRD). For the catalytic investigations, the material was powdered and transferred to the

reactor inside a glove box (Ar atmosphere, O₂ and H₂O below 1 ppm) to avoid significant contamination of the surface.

2.2. Quantum Chemical Calculations

Electronic structure calculation and bonding analysis in PdGa was carried out using the tight binding – linear muffin tin orbitals – atomic sphere approximation (TB-LMTO-ASA) program package.^[21] The following crystal structure model was used^[22]: space group $P2_13$ (no. 198), $a = 4.909$ Å; 4 Pd in Wyckoff position $4a$, xxx , $x = 0.14266$, 4 Ga in Wyckoff position $4a$, xxx , $x = -0.1568$. The Barth-Hedin exchange potential^[23] was employed for the LDA (local density approximation) calculations. The radial scalar-relativistic Dirac equation was solved to get the partial waves. Although the calculation within the atomic sphere approximation (ASA) should include corrections for the neglect of interstitial regions and partial waves of higher order,^[24] an addition of empty spheres was not necessary. The following radii of the atomic spheres were applied for the calculations for PdGa: $r(\text{Pd}) = 1.499$ Å, $r(\text{Ga}) = 1.529$ Å. A basis set containing Pd(5s,5p,4d) and Ga(4s,4p) orbitals was employed for a self-consistent calculation with Pd(4f) and Ga(4d) functions being down-folded. The calculations were performed spin-polarized.

The electron localization function (ELF, η)^[25] and the electron localizability indicator (ELI, Y)^[26] were evaluated with modules implemented within the TB-LMTO-ASA program package^[21]. The topology of ELI and ELF was analyzed using the program Basin^[27] with consecutive integration of the electron density in basins, which are bounded by zero-flux surfaces in the ELI (ELF) gradient field.

This procedure, similar to the one proposed by Bader for the electron density,^[28] allows to assign an electron count for each basin, revealing the basic information about the chemical bonding.

2.3. Characterization

In-situ high-pressure X-ray photoelectron spectroscopy (XPS) experiments were performed at beamline U49/2-PGM1 at BESSY (Berlin, Germany). Details of the setup have been published earlier^[29]. Briefly, the photoelectron spectrometer system uses a differentially pumped lens system between the sample cell and the electron analyzer, allowing XPS investigations during catalytic conditions in the mbar pressure range. For the measurements a dense pill of PdGa (8 mm in diameter, 1 mm thick) was produced by spark plasma sintering (SPS) at 873 K and 400 MPa in WC pressing tools. XPS investigations were performed in UHV (10^{-8} mbar) and *in-situ* conditions (1.0 mbar of H₂ (Westfalen Gas, 5.0) + 0.1 mbar of C₂H₂ (solvent free, Linde, 2.6) at 400 K). Gas-phase analysis was carried out using a quadrupole Balzers mass spectrometer connected by a leak

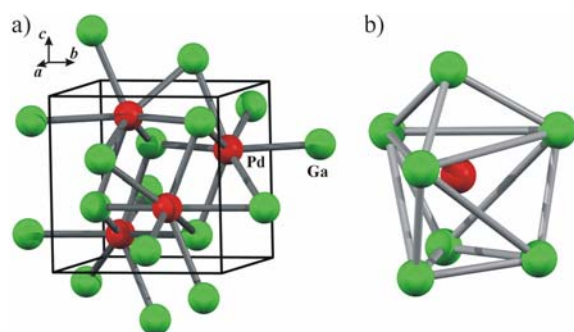


Figure 1: a) Crystal structure of PdGa (FeSi type, space group $P2_13$, $a = 4.909$ Å). b) Each Pd atom is surrounded by a shell of seven Ga atoms (Pd–Ga distances range between 2.543 and 2.712 Å, the shortest Pd–Pd distance is 3.016 Å).

valve to the experimental cell. The geometry of the XPS cell is inadequate to realize significant conversion – especially for SPS-pressed pills which feature a very low surface area. Thus, mass spectrometry was used to confirm that the reaction takes place.

Fourier transform infrared spectroscopy (FTIR) measurements were carried out using a Perkin-Elmer S 2000 spectrometer with a resolution of 4 cm^{-1} and an accumulation of 32 scans. PdGa powder was mixed with high-surface area silica (Degussa) and subsequently pressed into thin wafers. The sample was treated in a heatable section of the IR cell which was connected to a vacuum line with a residual pressure of 10^{-6} mbar. Presented are difference spectra obtained by subtraction of the spectrum of the treated sample in vacuum from the spectrum in presence of the probe molecule CO.

Catalytic investigations were conducted in a plug-flow reactor consisting of a quartz glass tube (inner diameter 7 mm, length 300 mm) which was equipped with a sintered glass frit to support the catalyst bed. Activity, selectivity and long-term stability were measured in a mixture of 0.5 % C_2H_2 , 5 % H_2 and 50 % C_2H_4 in helium (total flow of 30 ml/min) at 473 K. Gases were obtained from Westfalen Gas: 5 % of C_2H_2 (2.6) in He (4.6), H_2 (5.0), C_2H_4 (3.5) and He (5.0). The concentrations of the educts and products were monitored by a micro gas chromatograph (Varian CP 4900). A commercial Pd/ Al_2O_3 catalyst (Sigma-Aldrich 205710, 5 wt.-% Pd, BET surface: $114\text{ m}^2/\text{g}$, Pd surface $6\text{ m}^2/\text{g}$) was used as reference.

3. Results and Discussion

Single-phase material was obtained by melting the metals together. The obtained powder X-ray diffraction pattern is in accordance with the published data of PdGa^[30]. The crystal structure of PdGa (FeSi type) is displayed in Figure 1a. As has been pointed out above, isolated Pd atoms are required for the selective partial hydrogenation of acetylene and – as can be seen in Figure 1b – the Pd atoms

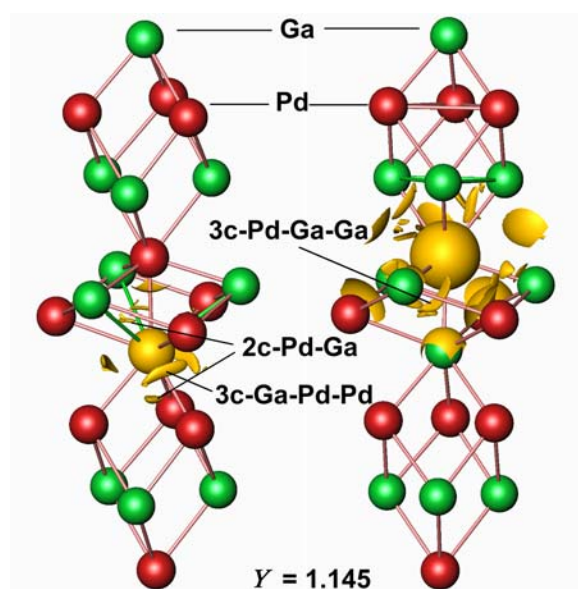


Figure 2: Electron localizability indicator (isosurface with $Y = 1.145$) and interatomic interactions in PdGa: (left) Positions of the ELI maxima in the vicinity of the gallium atoms; (right) ELI maxima around the palladium atoms.

in PdGa are well separated by the surrounding Ga shell. The Pd–Ga distances within the first shell are in the range of 2.543 Å to 2.712 Å. The separation results in a shortest Pd–Pd distance of 3.016 Å – an increase of almost 10 % compared to the distance in metallic Pd, viz. 2.751 Å^[31].

A further requirement for an effective catalyst is the presence of covalent bonding to stabilize the desired geometry under reaction conditions thus preventing the deactivation of the catalysts. In Fig. 2 the results of the quantum chemical calculation of the electron localizability indicator (ELI) are shown. As illustrated by the isosurface with ELI = 1.145 (Fig. 2), the inner shells of palladium and gallium atoms are non-structured, which suggests that the electrons of these shells do not participate relevantly in the bonding in the valence region. In turn, the valence region reveals strong structuring indicating the more directed (covalent) atomic interactions in PdGa. The local maxima appear mainly in the triangles between one gallium and two palladium atoms or between one palladium and two gallium atoms. The positions of the maxima can be interpreted as follows. Each gallium atom (Fig. 2, left) is participating in a two-centre (2c) interaction with the nearest palladium atom ($d = 2.543$ Å), three three-centre (3c) interactions Pd–Ga–Pd and three 3c interactions Ga–Pd–Ga. Each palladium atom (Fig. 2, right) is forming one 2c bond Pd–Ga, three Pd–Ga–Pd and three Ga–Pd–Ga bonds. No homoatomic interactions were found by ELI analysis. As a result a three-dimensional well ordered framework is formed indicating high structural stability in agreement with the high melting point of the compound (1318 K)^[32]. A more detailed analysis of the chemical bonding will be the subject of a forthcoming publication.

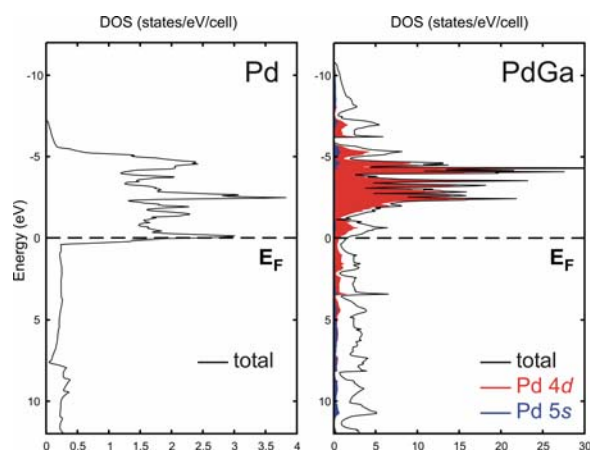


Figure 3: Electron density of states (DOS) of PdGa with the partial contributions of the 4d and 5s orbitals (right) in comparison to the DOS for elemental Pd (left).

In Fig. 3 the electron density of states (DOS) of PdGa and Pd metal with contributions of Pd 4d and Pd 5s orbitals are shown. Comparison of the two DOS clearly reveals that in case of elemental palladium the Pd 4d states lie in the vicinity of the Fermi level and are not completely filled, while in case of PdGa they are shifted below the Fermi level. For PdGa, the states close to the Fermi level are composed of Pd as well as Ga orbitals. The shift of the Pd 4d orbitals should have an influence on the adsorption properties of PdGa as will be demonstrated by FTIR.

As expected from the ELI, it could be shown by means of *in-situ* XRD and *in-situ* extended X-ray absorption fine structure spectroscopy (EXAFS) that PdGa indeed holds the necessary bulk stability under reaction conditions^[19]. Even though powder X-ray diffraction is sensitive to changes in the long range order and EXAFS can detect variations in the local environment, they are both bulk methods. Since catalysis takes place on the surface of the material, we were also interested in the behaviour of the surface, especially under reaction conditions. Therefore,

UHV and *in-situ* high pressure XPS as well as FTIR spectroscopy were employed to probe the surface.

UHV XPS measurements revealed a significant modification of the Pd electronic states in the intermetallic compound compared to Pd metal: the Pd3d_{5/2} peak is shifted by 1 eV to higher binding energy (Figure 4). Thus, the difference in the electronic structure of PdGa and metallic Pd is not only pronounced in the states close to the Fermi level (compare DOS, Figure 3) but also in the low lying Pd3d levels ($E \approx -336$ eV). This modification of the palladium electronic states in PdGa is likely caused by the presence of covalent bonding. A similar positive shift of Pd3d binding energy was observed for a Pd-Zn surface alloy, where the formation of intermetallic compounds can be expected^[33].

How is the electronic structure of Pd in PdGa affected by the reactive gases? To answer this question, high-pressure *in-situ* XPS was used to explore the surface electronic structure of PdGa during the partial hydrogenation of acetylene. The measurements, performed at ~1 mbar pressure, revealed a high stability of the Pd surface states (Figure 4). Neither shows the Pd3d_{5/2} peak a significant shift nor do additional components appear. This is in contrast to Pd metal for which the *in-situ* formation of an additional Pd component during 1-pentyne hydrogenation was detected recently^[34]. The formed component, which shows a higher binding energy (335.6 – 335.7 eV) than metallic palladium (335.0 eV), corresponds to a carbon-containing palladium surface phase. This phase was proposed to be responsible for the selective pentyne hydrogenation process instead of Pd metal^[34]. In the case of PdGa, the palladium electronic states are already changed due to the presence of intermetallic chemical bonding – leading to a binding energy of ~336.0 eV – so no further modification with carbon and/or hydrogen is necessary or possible to gain the catalytic properties. This results also in a suppression of the subsurface chemistry (incorporation of hydrogen or carbon) which is observed in the case of pure Pd^[34–37].

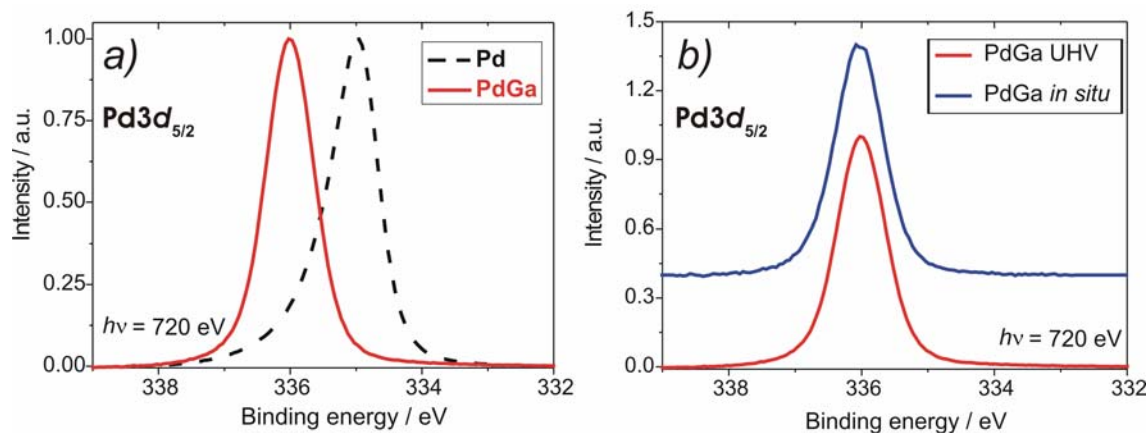


Figure 4:a) Comparison of the Pd3d_{5/2} UHV XPS spectra of metallic Pd and PdGa. The shift to higher binding energy for PdGa is clearly visible. b) Identical Pd3d_{5/2} spectra of PdGa in UHV and *in situ* conditions evidence no shift or additional components

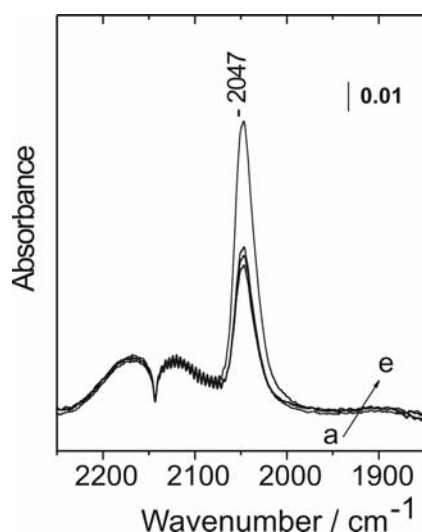


Figure 5: FTIR spectra of CO adsorbed on PdGa at room temperature. The sequence from *a* to *e* corresponds to increasing exposition times: immediately after introducing 50 mbar of CO (*a*), after 1, 5, 10 and 60 minutes (*e*).

The Ga2p and Pd3d XP spectra were measured at different photon energies of the X-ray beam in such a way that the kinetic energy of the produced photoelectrons (KE) was alike, thus allowing to obtain information for both elements from the same penetration depth. After correction for the sensitivity factors the Pd/Ga ratio was calculated to be equal to 0.9 for the very surface sensitive mode, KE = 150 eV. This is a strong argument that the bulk and the surface compositions of PdGa are identical.

Since the PdGa SPS pill was in contact with air, some carbon-containing species were adsorbed on the surface as was revealed by UHV XPS. *In-situ* measurements of the C1s XP spectrum (not shown) indicated the expected increase of surface carbon concentration due to adsorbed hydrocarbon species, but no significant shift or formation of additional carbon components was detected. Depth profiling of the pill – measurements were performed at different photon energies of the X-ray beam in order to get information from different penetration depths – was performed for Pd3d and C1s peaks. Peaks positions and shapes remain unaltered while the carbon content decreases monotonically with increasing penetration depth which confirms the absence of a carbon containing surface phase.

In the case of metallic palladium, hydrocarbon deposits and hydrocarbon decomposition with subsequent formation of carbonaceous deposits are regarded as the main reasons for deactivation of the catalyst^[38–40]. PdGa does not have adjacent Pd atoms which are necessary to form carbon deposits. Thus, the significantly enhanced long-term stability compared to metallic palladium can be attributed to geometric as well as electronic reasons (*vide infra*).

While XPS provides information about the electronic structure of the surface palladium sites, the local environment can be probed by CO adsorption using FTIR spec-

troscopy. Adsorption of CO on PdGa at room temperature results in the appearance of only one sharp band with a maximum at 2047 cm⁻¹ (Figure 5). This band was reproducible even after oxidation of the catalyst (200 mbar O₂ at 400 °C for 30 minutes and 60 minutes evacuation before CO adsorption at room temperature) which is in good agreement with the *in-situ* bulk^[19] and surface stability of PdGa. The observed band disappears easily after short evacuation of the sample at room temperature. Since CO molecules adsorbed on two or more Pd atoms reveal significantly higher stability compared to the linearly adsorbed CO on Pd^[41] we assign this band to CO adsorbed on Pd in on-top position. The shift of the observed band to lower wavenumbers – compared to CO on-top on metallic palladium (2080–2100 cm⁻¹)^[41] – may be due to the modification of the Pd electronic states by the covalent bonding in PdGa. In addition to the bands arising from on-top species, pronounced bands in the region of 1900–2000 cm⁻¹ are observed for metallic palladium, corresponding to CO molecules bridging neighboring Pd atoms^[41–43]. The absence of such species on PdGa is directly connected to the isolation of Pd active sites on the surface. Further insight can be gained by the coverage dependence of the vibration frequency. CO molecules adsorbed on-top on neighboring Pd atoms on palladium metal influence each other through dipole-dipole interactions resulting in a coverage-dependence of the frequency^[41;44]. No such shift was observed in the case of PdGa (Fig. 5). Together with the absence of bands due to bridging CO, this is a clear indication that the active sites of PdGa are really isolated.

Summarizing the XPS and FTIR results one can expect long-term stability and high selectivity for the PdGa catalyst in the partial hydrogenation of acetylene since only isolated and stable Pd sites are present on the surface.

Catalytic testing proved that this is the case. Activity, selectivity and long-term stability were determined in an excess of ethylene (C₂H₄/C₂H₂ ratio 100:1), thus simulating industrial conditions. Isothermal experiments were performed by heating the catalysts – 400 mg of PdGa and 0.1 mg Pd/Al₂O₃ for comparison – in helium to a temperature of 473 K followed by switching to the ethylene-rich feed (ratio C₂H₄/H₂/C₂H₂ = 100/10/1).

The obtained conversion of acetylene and the corresponding selectivity to ethylene are shown in Figure 6. During 20 hours on stream PdGa showed a stable conversion of 70 %, whereas Pd/Al₂O₃ exhibited a strong deactivation (from 100 % to 45 %). In addition to a high long-term stability, PdGa possessed a high and long-time stable selectivity of over 75 % compared to less than 20 % selectivity of Pd/Al₂O₃. It should be mentioned that the activity of the catalysts can not be compared as the large difference is a result of the very different surface areas.^[45]

As could be shown, our rational approach to a well-defined, stable and site-isolated catalyst is indeed working. Furthermore, due to the knowledge of the active species, we could show that isolated sites are responsible for the high selectivity and thus for the semi-hydrogenation of acetylene. Further improvement of the catalyst is possible,

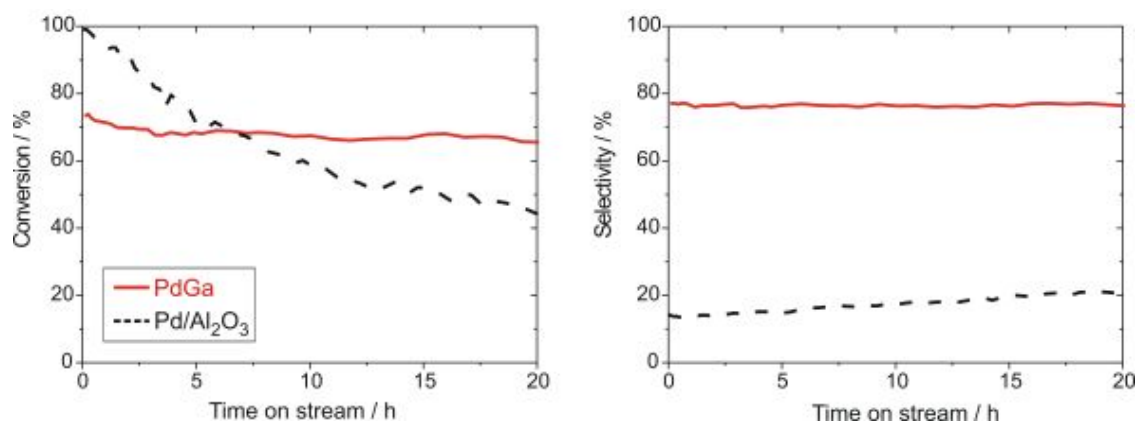


Figure 6: Catalytic data for the hydrogenation of acetylene to ethylene catalysed by PdGa (400 mg) and Pd/Al₂O₃ (0.1 mg) (see text for details). While the supported Pd exhibits low selectivity as well as strong deactivation with time on stream, PdGa possesses high and stable selectivity.

since the catalytic properties can be undoubtedly assigned to the compound PdGa, e.g., the dependence of the selectivity on the Pd-Pd distance in different intermetallic compounds can be investigated.

4. Conclusion

By applying a new and rational approach to well-defined, stable and site-isolated catalysts, it was possible to identify PdGa as highly selective and long-term stable catalyst for the semihydrogenation of acetylene.

Quantum chemical calculations and XPS measurements revealed a significant difference between the electronic structures of PdGa and Pd metal in combination with

covalent bonding detected by the ELI. By means of XPS and FTIR measurements it could be shown, that the surface only holds isolated Pd atoms, thus providing high selectivity and long-term stability – the latter most probably due to the absence of carbon deposits.

Utilizing our concept, it is not only possible to assign the catalytic properties to a specific compound, but also a further rational development is conceivable.

Acknowledgement

The authors thank BESSY for providing beamtime and continuing support during the XPS measurements.

References

- [1] M. Raney, US 1563587, **1925**.
- [2] M. Raney, US 1628190, **1927**.
- [3] S. Sane, J. M. Bonnier, J. P. Damon, J. Masson, *Appl. Catal.* **1984**, 9 69–83.
- [4] R. M. Nix, T. Rayment, R. M. Lambert, J. R. Jennings, G. Owen, *J. Catal.* **1987**, 106 216–234.
- [5] C. M. Hay, J. R. Jennings, R. M. Lambert, R. M. Nix, G. Owen, T. Rayment, *Appl. Catal.* **1988**, 37 291–304.
- [6] H. Imamura, W. E. Wallace, *Am. Chem. Soc. Div. Fuel Chem.* **1979**, 25 82–87.
- [7] J. E. France, W. E. Wallace, *Lanthan. Actin. Res.* **1988**, 2 165–180.
- [8] V. T. Coon, W. E. Wallace, R. S. Craig, in: *Rare Earths in Modern Science and Technology*, G. J. McCarthy, J. J. Rhyne (eds.), Plenum Press, New York, **1978**, 93–98.
- [9] M. Consonni, D. Jokic, D. Y. Murzin, R. Touroude, *J. Catal.* **1999**, 188 165–175.
- [10] F. Ammari, J. Lamotte, R. Touroude, *J. Catal.* **2004**, 221 32–42.
- [11] Y.-H. Chin, R. Dagle, J. Hu, A. C. Dohnalkova, Y. Wang, *Catal. Today* **2002**, 77 79–88.
- [12] A. Karim, T. Conant, A. Datye, *J. Catal.* **2006**, 243 420–427.
- [13] A. M. Doyle, S. K. Shaikhutdinov, H.-J. Freund, *J. Catal.* **2004**, 223 444–453.
- [14] S. K. Shaikhutdinov, M. Heemeier, M. Bäumer, T. Lear, D. Lennon, R. J. Oldman, S. D. Jackson, H.-J. Freund, *J. Catal.* **2001**, 200 330–339.
- [15] S. K. Shaikhutdinov, M. Frank, M. Bäumer, S. D. Jackson, R. J. Oldman, J. C. Hemminger, H.-J. Freund, *Catal. Lett.* **2002**, 80 115–122.
- [16] G.C. Bond, P.B. Wells, *J. Catal.* **1966**, 5 65–73.
- [17] M. Boström, Yu. Prots, Yu. Grin, *J. Solid State Chem.* **2006**, 179 2472–2478.
- [18] Yu. Grin, F. R. Wagner, M. Armbrüster, M. Kohout, A. Leithe-Jasper, U. Schwarz, U. Wedig, H. G. von Schnering, *J. Solid State Chem.* **2006**, 179 1707–1719.
- [19] J. Osswald, K. Kovnir, M. Armbrüster, R. E. Jentoft, R. Giedigkeit, T. Ressler, Y. Grin, R. Schlögl, *Angew. Chem. Int. Ed.* **2006**, submitted.
- [20] K. Kovnir, J. Osswald, M. Armbrüster, R. Giedigkeit, T. Ressler, Y. Grin, R. Schlögl, *Stud. Surf. Sci. Catal.* **2006**, 162 481–488.
- [21] O. Jepsen, A. Burkhardt, O. K. Andersen, The Program TB-LMTO-ASA. Version 4.7. Max-Planck-Institut für Festkörperforschung, Stuttgart, **1999**.
- [22] R. Giedigkeit, *PhD Thesis*, Technische Universität Dresden, **2007**.
- [23] U. Barth, L. Hedin, *J. Phys. C* **1972**, 5 1629–1642.
- [24] O. K. Andersen, *Phys. Rev. B* **1975**, 12 3060–3083.

- [25] A. Savin, H. J. Flad, J. Flad, H. Preuss, H. G. von Schnering, *Angew. Chem.* **1992**, 104 185–186; *Angew. Chem. Int. Ed. Engl.* **1992**, 31 185–187.
- [26] M. Kohout, *Int. J. Quantum Chem.* **2004**, 97 651–658.
- [27] M. Kohout, *Basin*. Version 2.3. Max-Planck-Institut für Chemische Physik fester Stoffe, Dresden, **2001**.
- [28] R. F. W. Bader, *Atoms in molecules: a quantum theory*. Oxford University Press, Oxford, **1999**.
- [29] H. Bluhm, M. Hävecker, A. Knop-Gericke, E. Kleimenov, R. Schlögl, D. Teschner, V. I. Bukhtiyarov, D. F. Ogletree, M. Salmeron, *J. Phys. Chem. B* **2004**, 108 14340–14347.
- [30] M. K. Bhargava, A. A. Gadalla, K. Schubert, *J. Less-Common Met.* **1975**, 42 69–76.
- [31] H. E. Swanson, E. Tatge, *Nat. Bureau Standards* **1953**, 359 21–22.
- [32] T. B. Massalski, in: *Binary Alloy Phase Diagrams*, Vol. 2, T. B. Massalski (ed.), ASM International, Materials Park, Ohio **1990**, 1836–1838.
- [33] J. A. Rodriguez, *J. Phys. Chem.* **1994**, 98 5758–5764.
- [34] D. Teschner, E. Vass, M. Hävecker, S. Zafeirotas, P. Schnörch, H. Sauer, A. Knop-Gericke, R. Schlögl, M. Chamam, A. Wootsch, A. S. Canning, J. J. Gamman, S. D. Jackson, J. McGregor, L. F. Gladden, *J. Catal.* **2006**, 242 26–37.
- [35] A. Borodzinski, G. C. Bond, *Catal. Rev.* **48** (2006) 91–144.
- [36] W. Palczewska, in Z. Paal, P. G. Denon (Eds.) *Hydrogen Effects In Catalysis*, Marcel Decker, New York, 1988, p. 372.
- [37] A. M. Doyle, S. K. Shaikhutdinov, S. D. Jackson, H. J. Freund, *Angew. Chem. Int. Ed.* **42** (2003) 5240–5243.
- [38] P. Albers, J. Pietsch, S. F. Parker, *J. Molec. Catal. A* **2001**, 173 275–286.
- [39] H. Arnold, F. Döbert, J. Gaube, in: *Handbook of Heterogeneous Catalysis*, G. Ertl, H. Knoerzinger, J. Weitkamp (eds.), VCH, Weinheim, **1997**, 2165.
- [40] A. Molnár, A. Sarkany, M. Varga, *J. Molec. Catal. A* **2001**, 173 185–221.
- [41] H. Unterhalt, G. Rupprechter, H.-J. Freund, *J. Phys. Chem. B* **2002**, 106 356–367.
- [42] D. Tessier, A. Rakai, F. Bozon-Verduraz, *J. Chem. Soc. Faraday Trans.* **1992**, 88 741–749.
- [43] E. W. Shin, C. H. Choi, K. S. Chang, Y. H. Na, S. H. Moon, *Catal. Today* **1998**, 44 137–143.
- [44] S. Bertarione, D. Scarano, A. Zecchina, V. Johanek, J. Hoffmann, S. Schauerermann, M. M. Frank, J. Libuda, G. Rupprechter, H.-J. Freund, *J. Phys. Chem. B* **2004**, 108 3603–3613.
- [45] The surface area of Pd/Al₂O₃ was 114 m²/g with a active Pd surface of 6 m²/g, and 0.1 mg of the catalyst reached a conversion of > 95 %. The surface area of PdGa was below the limit of conventional nitrogen BET measurements. However, after milling and chemical etching of the PdGa^[20] it possessed a higher surface area of ~ 2 m²/g. In order to reach similar acetylene conversion only 1.5 mg of PdGa was necessary, which clearly demonstrates that the surface activity of PdGa is similar to those of the supported Pd catalysts.